Structure of praseodymium and neodymium gallate glasses

Kamil Wezka[a], Anita Zeidler[a], Philip S. Salmon[a], Pinit Kidkhunthod[b], Adrian C. Barnes[b], Henry E. Fischer[c]

[a] *Department of Physics, University of Bath, Bath BA2 7AY, UK*
[b] *H.H. Wills Physics Laboratory, University of Bristol, Tyndall Avenue, Bristol BS8 1TL, UK*
[c] *Institut Laue-Langevin, 6 rue Jules Horowitz, BP 156, F-38042, Grenoble Cédex 9, France*

Abstract

The rare-earth gallate glasses $R_4Ga_6O_{15}$, where R denotes Pr or Nd, were prepared using an aerodynamic levitator and laser heating system. The structure was studied by applying the method of isomorphic substitution in neutron diffraction which allows for an identification of the gallium and rare-earth coordination environments. The results give a mean Ga-O coordination number of 4.2(1) at a distance of 1.85(2) Å and a mean R-O coordination number of 7.4(2) at a mean distance of 2.38(2) Å. The experimental results are consistent with a glass network built from GaO_4 tetrahedra and with the presence of GaO_6 octahedra at the 10(5)% level.

Keywords: Glass structure, neutron diffraction, aerodynamic levitation

1. Introduction

Rare-earth glasses with a small maximum phonon energy, *i.e.* with a low cut-off frequency in the vibrational density of states, are of interest as materials for infrared and infrared to visible upconversion lasers and for optical fibre amplifiers [1, 2, 3, 4, 5, 6, 7, 8]. It is difficult, however, to make suitable rare-earth containing oxide glasses owing to the high vibrational frequencies associated with the structural motifs of typical network glass formers such as SiO_2, GeO_2, B_2O_3 and P_2O_5 which lead to undesirable non-radiative losses from multiphonon relaxation. Gallate glasses have relatively low vibrational

frequencies and are chemically durable by comparison with their halide counterparts [1, 3, 4, 7, 8, 9]. These materials are therefore of interest as the host matrix for rare-earth ions and several of the optical properties of Pr^{3+} [3, 5], Nd^{3+} [3], Ho^{3+} [7], Er^{3+} [1, 2, 4] and Tm^{3+}/Yb^{3+} [8] doped multicomponent glasses have been examined.

It is desirable to understand the structure of these materials in order to develop *e.g.* non-phenomenological microscopic models for the interactions between the rare-earth ions and their mediation by the matrix material which effect losses from cross-relaxation and cooperative upconversion processes. Progress on this front is dependent on the provision of unambiguous experimental information about the relative distribution of the rare-earth ions and the structure of the glass matrix. This information can in principle be accessed, at the pair correlation function level, by means of diffraction methods through measurement of the (Faber-Ziman [10]) partial structure factors, $S_{\alpha\beta}(k)$, where k is the magnitude of the scattering vector. The accompanying experimental challenge is, however, formidable. For instance, a multicomponent glass containing n elements is described by $n(n+1)/2$ overlapping pair correlation functions [11].

In this paper we tackle the problem by applying the method of *isomorphic* substitution in neutron diffraction [12, 13, 14, 15, 16, 17] to study the structure of the rare-earth gallate glasses $(R_2O_3)_{0.4}(Ga_2O_3)_{0.6}$ or $R_4Ga_6O_{15}$, where R denotes Pr or Nd, prepared by quenching aerodynamically levitated liquid drops [18]. The Pr^{3+} and Nd^{3+} ions were chosen as isomorphic pairs since they are adjacent in the periodic table and they have comparable cation radii (1.126 Å *cf.* 1.109 Å for 8-fold coordination) [19] and Pettifor chemical parameters (0.70 *cf.* 0.6975) [20]. They also share a similar structural chemistry [21, 22] *e.g.* the rare-earth gallates $PrGaO_3$ and $NdGaO_3$ have a perovskite structure [23, 24, 25, 26, 27] while $Pr_4Ga_2O_9$ and $Nd_4Ga_2O_9$ also share a common crystal structure [28, 29]. By treating Pr^{3+} and Nd^{3+} as isomorphic pairs and by measuring the diffraction patterns of the glasses it is possible to probe separately the coordination environments of both the rare-earth and gallium atoms. The use of laser heating and containerless aerodynamic levitation enables three component rare-earth gallate glasses to be made, thus simplifying an interpretation of the neutron diffraction results. This preparation method also allows for the possibility of making glasses with novel opto-electronic and magneto-optical properties [30, 31, 32, 33, 34].

The paper is organised as follows. The essential theory required to understand the diffraction data is described in Sec. 2 and the experimental

details are outlined in Sec. 3. The results are presented in Sec. 4 and are then discussed in Sec. 5 by reference to the results obtained for several other rare-earth oxide glasses. Finally, the conclusions are summarised in Sec. 6.

2. Theory

In a neutron diffraction experiment on a gallate glass containing a paramagnetic rare-earth ion, the differential scattering cross-section per atom for unpolarised neutrons can be written as

$$\left(\frac{d\sigma}{d\Omega}\right)_{\text{total}} = \left(\frac{d\sigma}{d\Omega}\right)_{\text{mag}} + \left(\frac{d\sigma}{d\Omega}\right)_{\text{nucl}}. \tag{1}$$

For the glasses used in the present work, Pr^{3+} and Nd^{3+} both exhibit paramagnetism and the corresponding differential scattering cross-section $(d\sigma/d\Omega)_{\text{mag}}$ was calculated in the free ion approximation by using the scheme outlined in Ref. [12] where the radial integrals for Pr^{3+} and Nd^{3+} were taken from Refs. [35] and [36], respectively. The nuclear differential scattering cross-section is given by

$$\left(\frac{d\sigma}{d\Omega}\right)_{\text{nucl}} = F(k) + \sum_{\alpha=1}^{n} c_\alpha \left[b_\alpha^2 + b_{\text{inc},\alpha}^2\right] \left[1 + P_\alpha(k)\right] \tag{2}$$

where c_α, b_α and $b_{\text{inc},\alpha}$ denote the atomic fraction, coherent scattering length and incoherent scattering length of chemical species α, respectively, n is the number of different chemical species, and $P_\alpha(k)$ is an inelasticity correction [37]. The total structure factor is defined by [11]

$$F(k) = \sum_{\alpha=1}^{n} \sum_{\beta=1}^{n} c_\alpha c_\beta b_\alpha b_\beta \left[S_{\alpha\beta}(k) - 1\right] \tag{3}$$

where $S_{\alpha\beta}(k)$ is related to the partial pair distribution function $g_{\alpha\beta}(r)$ by the Fourier transform relation

$$g_{\alpha\beta}(r) - 1 = \frac{1}{2\pi^2 \, n_0 \, r} \int_0^\infty \mathrm{d}k \, k \, \left[S_{\alpha\beta}(k) - 1\right] \sin(kr), \tag{4}$$

n_0 is the atomic number density, and r is a distance in real space. The mean coordination number of atoms of type β, contained in a volume defined by

two concentric spheres of radii r_i and r_j centred on an atom of type α, is given by

$$\bar{n}_\alpha^\beta = 4\pi\, n_0\, c_\beta \int_{r_i}^{r_j} \mathrm{d}r\, r^2 g_{\alpha\beta}(r) \tag{5}$$

where r_i and r_j are often chosen to correspond to the minima on either side of a peak in $g_{\alpha\beta}(r)$.

The isomorphic substitution method is based on the assumption that glassy samples can be made that are structurally the same but differ only in the coherent neutron scattering length of one of the chemical species *e.g.* the rare-earth element. By making neutron diffraction experiments on two samples containing rare-earth atoms with contrasting scattering lengths, $b_R > b\,'_R$, it is possible to eliminate those correlations not involving R by forming the first order difference function [12, 15]

$$\begin{aligned} \Delta F_R(k) &\equiv {}^{R}F(k) - {}^{'R}F(k) \\ &= c_R^2 \left(b_R^2 - b^{2\prime}{}_R\right) \left[S_{RR}(k) - 1\right] \\ &+ \sum_{\alpha \neq R} 2 c_\alpha c_R b_\alpha \left(b_R - b\,'_R\right) \left[S_{R\alpha}(k) - 1\right]. \end{aligned} \tag{6}$$

The rare-earth to matrix atom (Ga or O) correlations may also be eliminated by forming the difference function

$$\begin{aligned} \Delta F(k) &\equiv {}^{R}F(k) - \frac{b_R}{b_R - b\,'_R} \Delta F_R(k) \\ &= -c_R^2 b_R b\,'_R \left[S_{RR}(k) - 1\right] \\ &+ \sum_{\alpha \neq R} \sum_{\beta \neq R} c_\alpha c_\beta b_\alpha b_\beta \left[S_{\alpha\beta}(k) - 1\right]. \end{aligned} \tag{7}$$

The real-space representations of $\Delta F_R(k)$ and $\Delta F(k)$, denoted by $\Delta G_R(r)$ and $\Delta G(r)$ respectively, are obtained from Eqs. (6) and (7) by replacing each $S_{\alpha\beta}(k)$ by the corresponding $g_{\alpha\beta}(r)$ (see Eq. (4)). The small r limiting values $\Delta G_R(r=0)$ and $\Delta G(r=0)$ follow from setting $g_{\alpha\beta}(r=0) = 0$.

3. Experimental procedure

The samples were prepared from Pr_6O_{11} (99.99%) or Nd_2O_3 (99.99%) and Ga_2O_3 (99.99%) that had been calcined in air at 1200 °C for $\simeq$ 24 h to remove water and any CO_2 prior to use. This heat treatment is necessary to

ensure that the samples do not spatter and vitrify more readily (see below). Finely powdered oxides were first mixed and compressed to make a pellet. The pellets containing neodymium were on average of smaller mass than those containing praseodymium in order to ensure the reliable reproduction of a glassy material. Each pellet was melted by heating to 2300 °C with an aerodynamic levitation and laser heating system using argon (99.999%) as the levitation gas [18]. The molten sample was maintained at this temperature for $\simeq$ 1 min, to minimise sample loss by evaporation, and was then quenched by instantaneously cutting the laser power to zero. The samples thus produced were roughly spherical with a mean diameter of $\simeq$ 2.2 mm for the green praseodymium glasses and $\simeq$ 1.8 mm for the purple neodymium glasses. The colour of these glasses is consistent with the presence of Pr^{3+} and Nd^{3+} ions [38]. Praseodymium gallate glasses prepared by using air as the levitation gas were dark reddish in colour, indicating the presence of Pr^{4+} ions. Cooling rates of 100 °C s^{-1} at 1400 °C for samples of 1.8 mm diameter and 80 °C s^{-1} at 1400 °C for samples of 2.2 mm diameter were estimated by using the methodology described in Ref. [39]. The mass of the glassy spheres was smaller than the mass of the starting pellets which was attributed to a preferential loss of Ga_2O_3. The composition of the glasses was therefore much closer to $(R_2O_3)_{0.40}(Ga_2O_3)_{0.60}$ or $R_4Ga_6O_{15}$ than to their nominal composition of $(R_2O_3)_{0.375}(Ga_2O_3)_{0.625}$ or $R_3Ga_5O_{12}$ which was chosen since it corresponds to the composition of yttrium aluminium garnet (YAG) [18]. The data were analysed using the former composition and, to help in assessing the effect of an error in the composition, the data were also analysed using the nominal composition. The mass densities of the samples at 23.7(1) °C were 6.017(3) and 6.190(6) g cm^{-3} for the praseodymium and neodymium glasses, respectively, as measured with a Quantachrome Ultrapycnometer 1200e using dry helium gas as the displacement fluid. The corresponding number densities are 0.0741(1) and 0.0754(1) $Å^{-3}$, respectively, and the mean value of 0.0748 $Å^{-3}$ was used in the data analysis.

The neutron diffraction experiments were made at room temperature ($\simeq$25 °C) using the D4c instrument at the Institut Laue-Langevin (ILL) with an incident neutron wavelength of 0.4961(1) Å [40]. Each sample was made from a collection of glassy spheres which were placed in a cylindrical vanadium can of 4.8 mm inner diameter and 0.1 mm wall thickness. Diffraction patterns were taken for each sample in its container, the empty container, the empty instrument, and a cylindrical vanadium rod of diameter 6.072(6) mm for normalization purposes. The intensity for a bar of neutron

absorbing $^{10}B_4C$ of dimensions comparable to the sample was also measured to account for the effect of the sample's attenuation on the background signal at small scattering angles [41]. Each complete diffraction pattern was built up from the intensities measured for different positions of the group of nine microstrip detectors. These intensities were saved at regular intervals to check the stability of the sample and instrument [42].

The neutron diffraction data were carefully corrected to yield the total structure factor for each sample and the usual self-consistency checks were performed [43]. The coherent neutron scattering lengths are $b_{\rm Pr}$ = 4.58(5), $b_{\rm Nd}$ =7.69(5), $b_{\rm Ga}$ =7.288(2) and $b_{\rm O}$ =5.803(4) fm [44]. In the case of $R_4Ga_6O_{15}$ glass, the weighting factors for the R-R, R-Ga and R-O partial structure factors in Eq. (6) are 9.8(2), 17.4(4) and 34.7(8) mbarn (1 barn = 10^{-28} m^2), respectively, while the weighting factors for the R-R, Ga-O, Ga–Ga and O-O partial structure factors in Eq. (7) are -9.0(4), 121.80(9), 30.59(2) and 121.2(2) mbarn, respectively.

4. Results

The total structure factors $F(k)$ measured for the $Pr_4Ga_6O_{15}$ and $Nd_4Ga_6O_{15}$ glasses are shown in Fig. 1 together with the calculated paramagnetic differential scattering cross sections for the Pr^{3+} and Nd^{3+} ions. There is good overall agreement between each $F(k)$ and the back Fourier transform of the corresponding total pair correlation function $G(r)$, after the small r oscillations are set to their calculated $G(r = 0)$ limit, which indicates that the data correction procedure has been properly applied [43]. The results show a significant contrast between the diffraction patterns for the glasses, in keeping with the different scattering lengths of the rare-earth ions. A small pre-peak appears in $^{\rm Pr}F(k)$ at $\simeq$ 1.23 Å^{-1} but not in $^{\rm Nd}F(k)$. By comparison, the principal peak in $^{\rm Nd}F(k)$ at 2.15(2) Å^{-1} appears as a much smaller feature in $^{\rm Pr}F(k)$ at 2.16(2) Å^{-1}. The next peak appears at 2.65(2) and 2.72(2) Å^{-1} for the praseodymium and neodymium glasses, respectively, while the peak in $^{\rm Nd}F(k)$ at 4.50(2) Å^{-1} is smaller by comparison with the corresponding feature in $^{\rm Pr}F(k)$ at 4.53(2) Å^{-1} and has a more pronounced small k shoulder at 3.85(2) Å^{-1}.

The total pair distribution functions $G(r)$ are shown in Fig. 2. By comparison with the crystal structures of RGaO$_3$ (R = Pr or Nd) [23, 24, 25, 26], $R_4Ga_2O_9$ [28, 29] (R = Pr or Nd), Nd_3GaO_6 [45, 46] and $Nd_3Ga_5O_{12}$ [47], the first peak in $^{\rm Pr}G(r)$ at 1.85(2) Å or in $^{\rm Nd}G(r)$ at 1.86(2) Å is attributed

to Ga-O correlations and its integration over the range $1.66 \leq r(\text{Å}) \leq 2.09$ gives a coordination number $\bar{n}^{\rm O}_{\rm Ga} = 4.2(1)$. The second peak in ${}^{\rm Pr}G(r)$ at 2.44(2) Å or in ${}^{\rm Nd}G(r)$ at 2.42(2) Å will have a strong contribution from R-O correlations and, in keeping with the larger coherent neutron scattering length of Nd, this peak is more intense for the neodymium gallate glass.

The measured difference functions $\Delta F_R(k)$ and $\Delta F(k)$ for the two glasses are presented in Fig. 3 and show a trough in $\Delta F_R(k)$ at $\simeq 1.31$ Å^{-1} and a pre-peak in $\Delta F(k)$ at $\simeq 1.56$ Å^{-1}. There is good overall agreement between each function and the back Fourier transform of the corresponding $\Delta G_R(r)$ or $\Delta G(r)$ function, after the small r oscillations are set to the $\Delta G_R(r = 0)$ or $\Delta G(r = 0)$ limiting value, which indicates that the data correction procedures have been properly applied [43]. The $\Delta G_R(r)$ and $\Delta G(r)$ functions are shown in Fig. 4 and confirm the assignment made to the first two peaks in the total pair distribution functions.

Integration of the first peak in $\Delta G(r)$ at 1.85(2) Å over the range $1.66 \leq r(\text{Å}) \leq 2.09$ gives $\bar{n}^{\rm O}_{\rm Ga} = 4.2(1)$ while integration of the first peak in $\Delta G_R(r)$ at 2.38(2) Å over the range $2.09 \leq r(\text{Å}) \leq 2.95$ gives $\bar{n}^{\rm O}_{R} = 7.4(2)$. The first peak position in $\Delta G(r)$ compares with typical Ga-O distances in GaO_4 tetrahedra of 1.80–1.86 Å [47, 48, 49]. The small peak in $\Delta G(r)$ at 2.15(2) Å could not be identified with typical Ga-O distances of 1.94–2.08 Å in GaO_6 octahedra [47, 48, 49] nor with typical Ga-Ga homopolar bond distances of 2.43–2.80 Å [50, 51, 52, 53, 54]. An analysis of the neutron diffraction data assuming a glass composition of $R_3Ga_5O_{12}$ did not change the first peak position in $\Delta G_R(r)$ or $\Delta G(r)$ and led to coordination numbers of $\bar{n}^{\rm O}_{\rm Ga} = 4.2(1)$ and $\bar{n}^{\rm O}_{R} = 7.7(2)$.

In crystalline rare-earth gallates the nearest-neighbour R-Ga and R-R distances are in the range 3.13–3.32 Å and 3.55–3.83 Å, respectively [23, 24, 25, 26, 28, 29, 45, 46, 47]. By comparison, the second peak in $\Delta G_R(r)$ occurs at 3.76(2) Å and has a shoulder on its small r side in the region 3.38–3.44 Å. This shoulder and the second peak in $\Delta G_R(r)$ are, therefore, likely to have contributions from the R-Ga and R-R correlations, respectively. The oxygen coordination numbers are $\bar{n}^{\rm Ga}_{\rm O} = 1.68(2)$ and $\bar{n}^{R}_{\rm O} = 1.97(2)$ which give an overall mean oxygen coordination number of $\bar{n}_{\rm O} = \bar{n}^{\rm Ga}_{\rm O} + \bar{n}^{R}_{\rm O} = 3.65(3)$. Three and four fold coordinated oxygen atoms are found in materials like crystalline $R_4Ga_2O_9$ (R = Nd or Sm) [29].

5. Discussion

The nearest-neighbour Ga-O distance $r_{\mathrm{GaO}} = 1.85(2)$ Å and coordination number $\bar{n}^{\mathrm{O}}_{\mathrm{Ga}} = 4.2(1)$ are consistent with a glass network built predominantly from GaO_4 tetrahedra [55, 56, 57]. The coordination number can be rationalised in terms of a mixture of tetrahedral GaO_4 and octahedral GaO_6 units in a ratio of 0.90(5):0.10(5) if both of these motifs are present in the glass, as in crystalline β-Ga_2O_3 [48, 49] and $Nd_3Ga_5O_{12}$ [47]. There is evidence for a mixture of GaO_4 and GaO_6 motifs in other gallate glasses such as Ga_2O_3-P_2O_5 [57], PbO-Ga_2O_3 [55] and Bi_2O_3-Ga_2O_3 [55]. Nuclear magnetic resonance experiments using the ^{71}Ga nucleus would provide additional information on the nature of the Ga centered units that are present, at least in the case of glasses containing non-paramagnetic rare-earth ions such as La^{3+} [58]. For regular GaO_4 tetrahedra, an O-O distance $r_{\mathrm{OO}} = \sqrt{8/3}\ r_{\mathrm{GaO}} = 3.02$ Å is expected. This distance is comparable to the position of the second peak in $\Delta G(r)$ at 3.03(2) Å. In crystalline rare-earth gallates the nearest-neighbour Ga-Ga distances are 3.50 Å for $Nd_3Ga_5O_{12}$ [47], 3.47–3.56 Å for $R_4Ga_2O_9$ (R = Pr or Nd) [28, 29], 3.84–3.86 Å for $RGaO_3$ (R = Pr or Nd) [23, 24, 25, 26], and 5.23 Å for Nd_3GaO_6 [45, 46].

We note that the same praseodymium gallate glass has previously been investigated by using a combination of neutron diffraction and extended x-ray absorption fine structure (EXAFS) spectroscopy and the data were interpreted by using a combination of molecular dynamics and reverse Monte Carlo modeling methods [59]. In this work, the data were treated by assuming the nominal composition of $(Pr_2O_3)_{0.375}(Ga_2O_3)_{0.625}$ whereas the actual glass composition is closer to $(Pr_2O_3)_{0.40}(Ga_2O_3)_{0.60}$ (see section 3). The reverse Monte Carlo results show a network made predominantly from corner sharing GaO_4 tetrahedra and give a mean rare-earth coordination number of $\bar{n}^{\mathrm{O}}_{\mathrm{Pr}} = 6.7(1)$.

The nearest-neighbour R-O distance of 2.38(2) Å and coordination number $\bar{n}^{\mathrm{O}}_{R} = 7.4(2)$ obtained from the present work are in keeping with the values found for other oxide glasses containing large R^{3+} ions. For example, the method of isomorphic substitution in neutron diffraction has been used to investigate the structure of $(R_2O_3)_{0.218}(Al_2O_3)_{0.076}(P_2O_5)_{0.706}$ glass, where R denotes the large rare-earth La or Ce, and the results give $r_{RO} = 2.50(2)$ Å with $\bar{n}^{\mathrm{O}}_{R} = 7.5(2)$ [15, 17]. The same experimental method has also been applied to study the structure of $(R_2O_3)_{0.230}(Al_2O_3)_{0.069}(P_2O_5)_{0.701}$ glass, where R denotes the small rare-earth Dy or Ho, and the results give

a reduced nearest-neighbour distance $r_{RO} = 2.27(2)$ Å with $\bar{n}_R^O = 6.7(1)$ [14, 16, 17]. These results for the nearest-neighbour R-O parameters follow from the lanthanide contraction [21] and are in keeping with those obtained for other rare-earth phosphate glasses by using diffraction [60, 61, 62] and EXAFS spectroscopy [63] methods. For example, in the metaphosphate glasses $(Pr_2O_3)_{0.25}(P_2O_5)_{0.75}$ and $(Nd_2O_3)_{0.25}(P_2O_5)_{0.75}$ the nearest-neighbour R-O distances are 2.43(2) and 2.41(2) Å with corresponding coordination numbers of 6.8(3) and 6.9(3), respectively [61]. The non integer R-O coordination numbers are consistent with a distribution of rare-earth centred coordination polyhedra.

6. Conclusions

The method of isomorphic substitution in neutron diffraction was applied to study the structure of the rare-earth gallate glasses $R_4Ga_6O_{15}$, where R denotes Pr or Nd, as prepared by using a laser heating and aerodynamic levitation method. The results are consistent with a glass network made predominantly from GaO_4 tetrahedra in which R^{3+} ions reside with a mean R-O coordination number of 7.4(2). GaO_6 octahedra may also be present at the 10(5)% level.

Acknowledgments

We gratefully thank Alain Bertoni (Grenoble) for help with the neutron diffraction experiments and the EPSRC for financial support and for providing its Chemical Database Service. PK would like to thank the Royal Thai Government for financial support.

References

[1] S. Tanabe, K. Hirao, N. Soga, J. Non-Cryst. Solids 122 (1990) 79.

[2] X. Zou, T. Izumitani, J. Non-Cryst. Solids 162 (1993) 68.

[3] H. Takebe, K. Yoshino, T. Murata, K. Morinaga, J. Hector, W. S. Brocklesby, D. W. Hewak, J. Wang, D. N. Payne, Appl. Optics 36 (1997) 5839.

[4] S. Q. Man, E. Y. B. Pun, P. S. Chung, Appl. Phys. Lett. 77 (2000) 483.

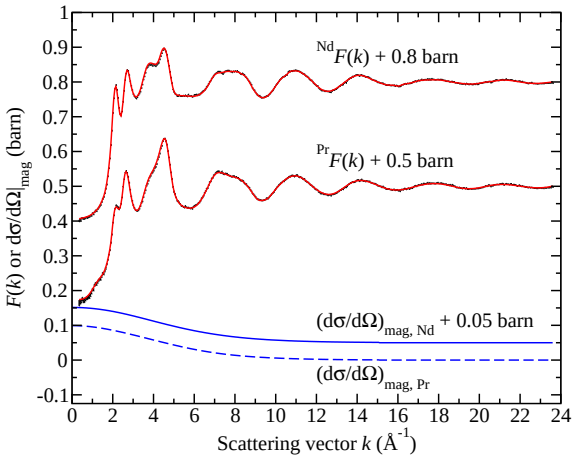

Figure 1: The measured total structure factors $F(k)$ for $Pr_4Ga_6O_{15}$ and $Nd_4Ga_6O_{15}$ glass. The dark solid (black) vertical bars represent the measured data points with statistical errors and the light solid (red) curves are the back Fourier transforms of the corresponding total pair distribution functions $G(r)$ given by the solid (black) curves in Fig. 2 where the oscillations at r values smaller than the distance of closest approach between the centres of two atoms are set to the calculated $G(r = 0)$ limit. For all of the functions the back Fourier transforms are indistinguishable from the data points at most k values. The dark solid (blue) and dark broken (blue) curves show the calculated paramagnetic differential scattering cross sections for the Nd^{3+} and Pr^{3+} ions, respectively.

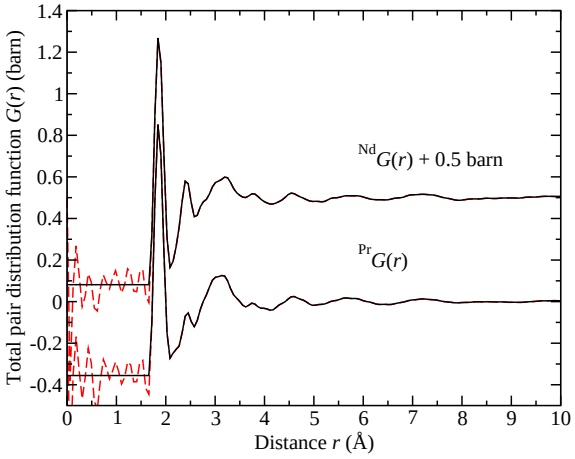

Figure 2: The total pair distribution functions $G(r)$ for $Pr_4Ga_6O_{15}$ and $Nd_4Ga_6O_{15}$ glass, as obtained by spline fitting and Fourier transforming the corresponding $F(k)$ functions shown in Fig. 1 by the points with error bars. The solid dark (black) curves show the $G(r)$ functions after the small r oscillations are set to the appropriate $G(r = 0)$ limiting value. The broken (red) curves show the extent of the small r oscillations.

[5] S. Q. Man, E. Y. B. Pun, P. S. Chung, J. Opt. Soc. Am. B 17 (2000) 23.

[6] M. C. Gonçalves, L. F. Santos, R. M. Almeida, C. R. Chimie 5 (2002) 845.

[7] G. A. Kumar, A. Martinez, E. Mejia, J. G. Eden, J. Alloys Compds. 365 (2004) 117.

[8] Q. Y. Zhang, T. Li, Z. H. Jiang, X. H. Ji, S. Buddhudu, Appl. Phys. Lett. 87 (2005) 171911.

[9] W. H. Dumbaugh, J. C. Lapp, J. Am. Ceramic Soc. 75 (1992) 2315.

[10] T. E. Faber, J. M. Ziman, Phil. Mag. 11 (1965) 153.

[11] H. E. Fischer, A. C. Barnes, P. S. Salmon, Rep. Prog. Phys. 69 (2006) 233.

[12] J. C. Wasse and P. S. Salmon, J. Phys.: Condens. Matter 11 (1999) 1381.

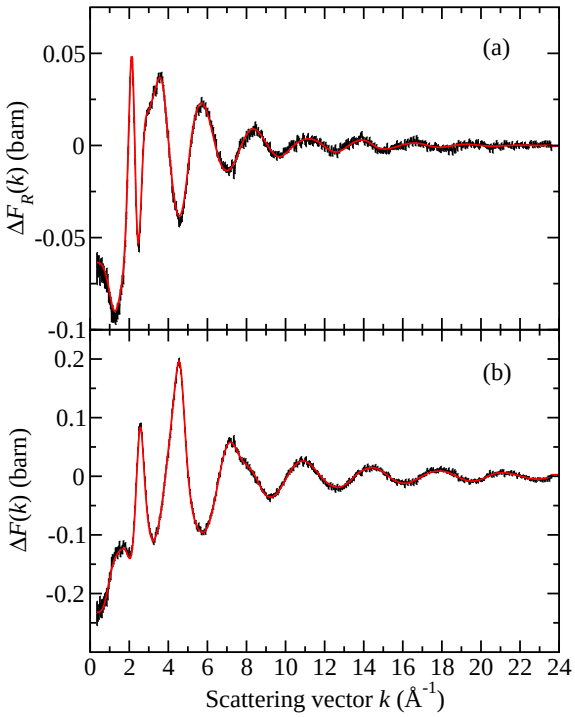

Figure 3: The measured difference functions (a) $\Delta F_R(k)$ and (b) $\Delta F(k)$ for glassy $R_4Ga_6O_{15}$ where R represents Pr or Nd. The vertical bars represent the measured data points with statistical errors and the light solid (red) curves are the back Fourier transforms of the corresponding real space difference functions $\Delta G_R(r)$ and $\Delta G(r)$ given by the solid (black) curves in Fig. 4 where the oscillations at r values smaller than the distance of closest approach between the centres of two atoms are set to the calculated $\Delta G_R(r = 0)$ or $\Delta G(r = 0)$ limit.

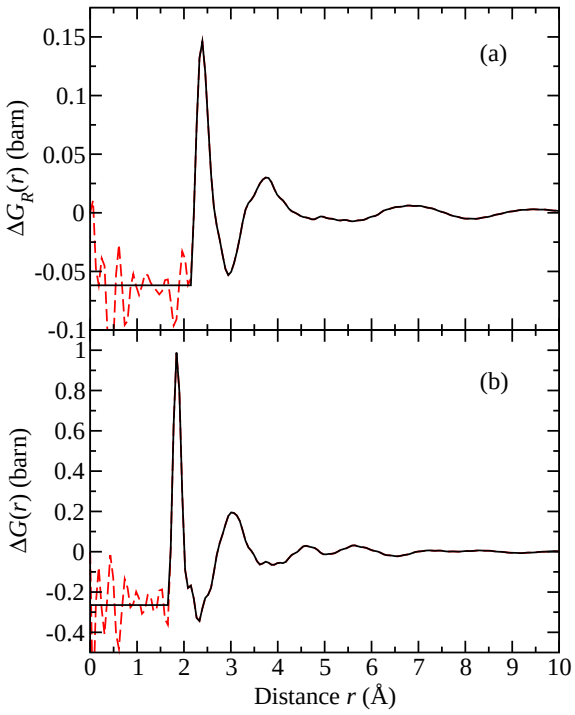

Figure 4: The measured difference functions (a) $\Delta G_R(r)$ and (b) $\Delta G(r)$ for glassy $R_4Ga_6O_{15}$, where R represents Pr or Nd, as obtained by spline fitting and Fourier transforming the corresponding difference functions $\Delta F_R(k)$ and $\Delta F(k)$ shown in Fig. 3 by the points with error bars. The solid dark (black) curves show $\Delta G_R(r)$ and $\Delta G(r)$ after the small r oscillations are set to the appropriate $\Delta G_R(r = 0)$ or $\Delta G(r = 0)$ limiting value. The broken (red) curves show the extent of the small r oscillations.

[13] J. C. Wasse, P. S. Salmon, R. G. Delaplane, J. Phys.: Condens. Matter 12 (2000) 9539.

[14] R. A. Martin, P. S. Salmon, H. E. Fischer, G. J. Cuello, Phys. Rev. Lett. 90 (2003) 185501.

[15] R. A. Martin, P. S. Salmon, C. J. Benmore, H. E. Fischer, G. J. Cuello, Phys. Rev. B 68 (2003) 054203.

[16] R. A. Martin, P. S. Salmon, H. E. Fischer, G. J. Cuello, J. Phys.: Condens. Matter 15 (2003) 8235.

[17] R. A. Martin, P. S. Salmon, H. E. Fischer, G. J. Cuello, J. Non-Cryst. Solids 345-346 (2004) 208.

[18] L. B. Skinner, A. C. Barnes, P. S. Salmon, W. A. Crichton, J. Phys.: Condens. Matter 20 (2008) 205103.

[19] R. D. Shannon, Acta Crystallogr. A 32 (1976) 751.

[20] D. G. Pettifor, J. Phys. C: Solid State Phys. 19 (1986) 285.

[21] T. Moeller, The Chemistry of the Lanthanides, Oxford, Pergamon Press, 1973.

[22] A. F. Wells, Structural Inorganic Chemistry, 5th ed. Oxford, Clarendon Press, 1984.

[23] W. Marti, P. Fischer, F. Altorfer, H. J. Scheel, M. Tadin, J. Phys.: Condens. Matter 6 (1994) 127.

[24] L. Vasylechko, L. Akselrud, W. Morgenroth, U. Bismayer, A. Matkovskii, D. Savytskii, J. Alloys Compds. 297 (2000) 46.

[25] L. Vasylechko, Ye. Pivak, A. Senyshyn, D. Savytskii, M. Berkowski, H. Borrmann, M. Knapp, C. Paulmann, J. Solid State Chem. 178 (2005) 270.

[26] R. J. Angel, J. Zhao, N. L. Ross, C. V. Jakeways, S. A. T. Redfern, M. Berkowski, J. Solid State Chem. 180 (2007) 3408.

[27] L. Vasylechko, A. Senyshyn, U. Bismayer, in: K. A. Gschneidner, Jr., J.-C. Bünzli, V. K. Pecharsky (Eds.), Handbook on the Physics and Chemistry of Rare Earths, vol. 39, Amsterdam, Elsevier, 2009, p. 113.

[28] Th. M. Gesing, R. Uecker, J.-C. Buhl, Z. Kristallogr. - New Crystal Structures 214 (1999) 431.

[29] F. S. Liu, Q. L. Liu, J. K. Liang, G. B. Song, J. Luo, L. T. Yang, Y. Zhang, G. H. Rao, J. Alloys Compds. 381 (2004) 26.

[30] J. K. R. Weber, J. J. Felten, B. Cho, P. C. Nordine, Nature 393 (1998) 769.

[31] C. J. Benmore, J. K. R. Weber, S. Sampath, J. Siewenie, J. Urquidi, J. A. Tangeman, J. Phys.: Condens. Matter 15 (2003) S2413.

[32] L. B. Skinner, A. C. Barnes, W. A. Crichton, J. Phys.: Condens. Matter 18 (2006) L407.

[33] A. Masuno, H. Inoue, J. Yu, Y. Arai, F. Otsubo, Adv. Mater. Research 39-40 (2008) 243.

[34] J. Yu, S. Kohara, K. Itoh, S. Nozawa, S. Miyoshi, Y. Arai, A. Masuno, H. Taniguchi, M. Itoh, M. Takata, T. Fukunaga, S. Koshihara, Y. Kuroiwa, S. Yoda, Chem. Mater. 21 (2009) 259.

[35] E. J. Lisher, J. B. Forsyth, Acta Crystallogr. A 27 (1971) 545.

[36] P. J. Brown, in: A. J. C. Wilson (Ed.) International Tables for Crystallography vol C, Dordrecht, Kluwer, 1995, p. 391.

[37] J. L. Yarnell, M. J. Katz, R. G. Wenzel, S. H. Koenig, Phys. Rev. A 7 (1973) 2130.

[38] K. Binnemans, C. Görller-Walrand, Chem. Phys. Lett. 235 (1995) 163.

[39] A. C. Barnes, L. B. Skinner, P. S. Salmon, A. Bytchkov, I. Pozdnyakova, T. O. Farmer, H. E. Fischer, Phys. Rev. Lett. 103 (2009) 225702.

[40] H. E. Fischer, G. J. Cuello, P. Palleau, D. Feltin, A. C. Barnes, Y. S. Badyal, J. M. Simonson, Appl. Phys. A 74 (2002) S160.

[41] H. Bertagnolli, P. Chieux, M. D. Zeidler, Mol. Phys. 32 (1976) 759.

[42] J. F. Jal, C. Mathieu, P. Chieux, J. Dupuy, Phil. Mag. B 62 (1990) 351.

[43] P. S. Salmon, S. Xin, H. E. Fischer, Phys. Rev. B 58 (1998) 6115.

[44] V. F. Sears, Neutron News 3 (1992) 26.

[45] F. S. Liu, Q. L. Liu, J. K. Liang, L. T. Yang, G. B. Song, J. Luo, G. H. Rao, J. Solid State Chem. 177 (2004) 1796.

[46] W. G. Zeier, I. P. Roof, M. D. Smith, H.-C. zur Loye, Solid State Sci. 11 (2009) 1965.

[47] H. Sawada, J. Solid State Chem. 132 (1997) 300.

[48] S. Geller, J. Chem. Phys. 33 (1960) 676.

[49] J. Åhman, G. Svensson, J. Albertsson, Acta Crystallogr. C 52 (1996) 1336.

[50] M. C. Bellissent-Funel, P. Chieux, D. Levesque, J. J. Weis, Phys. Rev. A 39 (1989) 6310.

[51] A. Di Cicco, A. Filipponi, J. Non-Cryst. Solids 156-158 (1993) 102.

[52] S. Wei, H. Oyanagi, W. Liu, T. Hu, S. Yin, G. Bian, J. Non-Cryst. Solids 275 (2000) 160.

[53] F. J. Bermejo, I. Bustinduy, S. J. Levett, J. W. Taylor, R. Fernández-Perea, C. Cabrillo, Phys. Rev. B 72 (2005) 104103.

[54] H. G. von Schnering, R. Nesper, Acta Chemica Scandinavica 45 (1991) 870.

[55] F. Miyaji, T. Yoko, J. Jin, S. Sakka, T. Fukunaga, M. Misawa, J. Non-Cryst. Solids 175 (1994) 211.

[56] A. C. Hannon, J. M. Parker, B. Vessal, J. Non-Cryst. Solids 196 (1996) 187.

[57] U. Hoppe, D. Ilieva, J. Neuefeind, Z. Naturforsch. A 57 (2002) 709.

[58] F. Miyaji, K. Tadanaga, T. Yoko, S. Sakka, J. Non-Cryst. Solids 139 (1992) 268.

[59] P. Kidkhunthod, A. C. Barnes, J. Phys.: Conf. Series 190 (2009) 012076.

[60] J. M. Cole, E. R. H. van Eck, G. Mountjoy, R. J. Newport, T. Brennan, G. A. Saunders, J. Non-Cryst. Solids 11 (1999) 9165.

[61] U. Hoppe, R. K. Brow, D. Ilieva, P. Jóvári, A. C. Hannon, J. Non-Cryst. Solids 351 (2005) 3179.

[62] A. C. Wright, J. M. Cole, R. J. Newport, C. E. Fisher, S. J. Clarke, R. N. Sinclair, H. E. Fischer, G. J. Cuello, Nucl. Instrum. Methods Phys. Res. A 571 (2007) 622.

[63] D. T. Bowron, G. A. Saunders, R. J. Newport, B. D. Rainford, H. B. Senin, Phys. Rev. B 53 (1996) 5268.